Dependence of kinetic friction on velocity: Master equation approach

O.M. Braun*

Institute of Physics, National Academy of Sciences of Ukraine, 46 Science Avenue, 03028 Kiev, Ukraine

M. Peyrard†

Laboratoire de Physique de l'Ecole Normale Supérieure de Lyon, 46 Allée d'Italie, 69364 Lyon Cédex 07, France
(Dated: January 20, 2013)

We investigate the velocity dependence of kinetic friction with a model which makes minimal assumptions on the actual mechanism of friction so that it can be applied at many scales provided the system involves multi-contact friction. Using a recently developed master equation approach we investigate the influence of two concurrent processes. First, at a nonzero temperature thermal fluctuations allow an activated breaking of contacts which are still below the threshold. As a result, the friction force monotonically increases with velocity. Second, the aging of contacts leads to a decrease of the friction force with velocity. Aging effects include two aspects: the delay in contact formation and aging of a contact itself, i.e., the change of its characteristics with the duration of stationary contact. All these processes are considered simultaneously with the master equation approach, giving a complete dependence of the kinetic friction force on the driving velocity and system temperature, provided the interface parameters are known.

I. INTRODUCTION

Almost three centuries ago Charles Coulomb (1736-1806) discovered that kinetic friction does not depend on the sliding velocity [1]. Later, more careful experiments showed that this law is only approximately valid [2–7]. Friction does depend on the sliding velocity, but this dependence is far from universal: some measurements find an increase when velocity increases, while others find a decay [8–10] or even a more complex non-monotonous behavior [2]. A logarithmic dependence, often quoted, has been found for two extreme scales, friction at the tip of an AFM (see for instance [8, 9, 11–13]) or at the scale of a fault in the earth crust [10], but it is often only approximate and observed in a fairly narrow velocity range. Therefore understanding the velocity dependence of kinetic friction is still an open problem, and what makes it difficult is that several phenomena contribute, the thermal depining of contacts, their aging, and the delay in contact formation.

In this study we investigate the velocity dependence of friction with a model that includes these three contributions and makes minimal assumptions on the actual mechanism of friction so that it can be applied at many scales provided the system involves multi-contact friction. Our aim is to elucidate the respective role of these three contributions to the velocity dependence of friction and to provide analytical treatments in some limits, or simple numerical approaches that allow the investigation of a velocity range that may span many orders of magnitude.

At the most fundamental level multi-contact friction can be described as resulting a succession of breaking and formation of local contacts which possess a distribution of breaking thresholds. This viewpoint was first applied to describe earthquakes [14, 15] and then adopted to friction by Persson [16].

We recently developed a master equation (ME) approach to describe the breaking and attachment events [17, 18]. It splits the analysis in two independent parts: (i) the calculation of the friction force, given by the master equation provided the statistical properties of the contacts are known, and (ii) the study of the properties of the contact themselves, which is system dependent. This method is very general and allows us to calculate the velocity dependence of friction, which results from the interplay of two concurrent processes. First, at a nonzero temperature thermal fluctuations allow an activated breaking of contacts which are still below their mechanical breaking threshold. This phenomenon leads to a monotonic increase of the friction force F with the velocity v. Second, the aging of contacts [19–21] leads to a decrease of the friction force with velocity. It includes two processes: the delay in contact formation, i.e., time lag between contact breaking and re-making [18, 20–23], and the aging of a contact itself, i.e., the change of its characteristics with the time of stationary contact. To incorporate the latter effect, the master equation must be completed by an equation for the evolution of static thresholds.

In earlier studies [17, 18] we considered thermal and aging effects separately, to set up the method. However, to relate the results to experiments, both contributions must be taken into account simultaneously. This is the aim of the present paper, which is organized as follows. Section II is a brief review of the mas-

*E-mail: obraun.gm@gmail.com; Web: http://www.iop.kiev.ua/~obraun
†E-mail: Michel.Peyrard@ens-lyon.fr

ter equation approach. Section III discusses temperature effects. Whereas our earlier work [18] focussed on time-dependent phenomena to analyze stick-slip, here we concentrate on the steady-state case (constant velocity). This allows us to proceed further and derive explicit expressions for the influence of temperature. Then Sec. IV introduces the second effect, the aging of the contacts. It first summarizes the method introduced earlier and its main results [18], which only considered the $T = 0$ case, and then studies the combined influence of aging and temperature fluctuations. Section V adds the influence of the delay in contact formation after breaking, to get the full picture, allowing us to compute the velocity dependence of friction. Section VI discusses all those results in the context of experimental data. The difficulty to apply the theory to actual experiments is to properly assess the values of the parameters that enter in the theoretical expressions, and not simply try to fit experimental curves, which would not be very significant owing to the number of parameters which are involved. Therefore Sec. VI focusses on this assessment. Finally, Sec. VII concludes the paper with a discussion of perspectives for its further development.

II. MASTER EQUATION

The earthquake (EQ) model is the most generic model for friction due to multiple contacts at an interface. The sliding interface is treated as a set of N_c "contacts" which deform elastically with the average rigidity k. The contacts represent, for example, asperities for the interface of rough surfaces [24], or patches of lubricant or its domains ("solid islands" [25]) in the case of lubricated friction. The ith contact connects the slider and the bottom substrate through a spring of elastic constant k_i. When the slider moves, the position of the contact point changes, and the contact's spring elongates or shortens, so that the slider experiences the force $-F = \sum f_i$ from the interface, where $f_i = k_i x_i$ and $x_i(t)$ is the spring length. The contacts are coupled frictionally to the slider. Namely, as long as the force $|f_i|$ is below a certain threshold f_{si} (corresponding to the onset of plastic flow of the entangled asperity, or to local shear-induced melting of the boundary lubrication layer), this contact i moves together with the slider. When the force exceeds the threshold, the contact breaks, and then re-attaches again in the unstressed state after some delay time τ. Thus with every contact we may associate the threshold value f_{si}, which takes random values from a distribution $\widetilde{P}_c(f)$ having a mean value f_s. The spring constants are related to the threshold forces by the relationship $k_i = k (f_{si}/f_s)^{1/2}$, because the value of the static threshold is proportional to the area A_i of the given contact, while the transverse rigidity k_i is proportional to contact's size, $k_i \propto \sqrt{A_i}$. When a contact is formed again (re-attached to the slider), new values for its parameters have to be assigned.

Rather than studying the evolution of the EQ model by numerical simulation it is possible to describe it analytically [17, 18]. Let $P_c(x)$ be the normalized probability distribution of values of the thresholds x_{si} at which contacts break; it is coupled with the distribution of threshold forces by the relationship $P_c(x)\,dx = \widetilde{P}_c(f)\,df$. To describe the evolution of the model, we introduce the distribution $Q(x; X)$ of the stretchings x_i when the bottom of the solid block is at a position X. Let us consider a small displacement $\Delta X > 0$ of the bottom of the sliding block. It induces a variation of the stretching x_i of the contacts which has the same value ΔX for all contacts (here we neglect the elastic deformation of the block). The displacement X leads to three kinds of changes in the distribution $Q(x; X)$: first, there is a shift due to the global increase of the stretching of the asperities; second, some contacts break because their stretching exceeds the maximum value that they can withstand; and third, those broken contacts form again, at a lower stretching, after a slip at the scale of the asperities, which locally reduces the tension within the corresponding asperities. These three contributions can be written as a master equation for $Q(x; X)$:

$$\left[\frac{\partial}{\partial x} + \frac{\partial}{\partial X} + P(x) \right] Q(x; X) = R(x)\,\Gamma(X), \quad (1)$$

where $P(x)\,\Delta X$ describes the fraction of contacts that break when the slider position changes from X to $X + \Delta X$. At zero temperature $P(x)$ is coupled with the threshold distribution $P_c(x)$ by the relationship [17, 18]

$$P(x) = P_c(x)/J_c(x), \quad J_c(x) = \int_x^\infty d\xi P_c(\xi). \quad (2)$$

The function $\Gamma(X)$ in Eq. (1) describes the contacts that form again after breaking,

$$\Gamma(X) = \int_{-\infty}^\infty d\xi\, P(\xi)\, Q(\xi; X) \quad (3)$$

(the delay time is neglected at this stage), and $R(x)$ is the (normalized) distribution of stretchings for newborn contacts. Then, the friction force is given by

$$F(X) = N_c\, k \int_{-\infty}^\infty dx\, x\, Q(x; X). \quad (4)$$

The evolution of the system in the quasi-static limit where inertia effects are neglected shows that, in the long term, the initial distribution approaches a stationary distribution $Q_s(x)$ and the total force F becomes independent of X. This statement is valid for any distribution $P_c(x)$ except for the singular case of $P_c(x) = \delta(x - x_s)$.

In the present work we concentrate on the steady state (smooth sliding). In what follows we use $R(x) = \delta(x)$ for simplicity. The steady-state solution of Eq. (1) is

$$Q(x) = \Theta(x)E_P(x)/C[P], \quad (5)$$

where $\Theta(x)$ is the Heaviside step function ($\Theta(x) = 1$ for $x \geq 0$ and 0 otherwise), $E_P(x) = \exp[-U(x)]$, $U(x) =$

$\int_0^x d\xi\, P(\xi)$, and $C[P] = \int_0^\infty dx\, E_P(x)$. Note also that, in the steady state,

$$\Gamma = 1/C[P]\,, \qquad (6)$$

because $\int_0^\infty d\xi\, P(\xi) E_P(\xi) = \int_0^\infty dU\, e^{-U} = 1$.

The distribution $\widetilde{P}_c(f)$ can be estimated for the contact of rough surfaces [18, 24] as well as for the contact of polycrystal substrates [18, 26]: its general shape may be approximated by the function

$$\widetilde{P}_c(f) \propto f^n \exp(-f/f_*)\,, \qquad (7)$$

where $n \geq 0$ depends on the nature of the interface. Then, the distribution $P_c(x)$ can be related to the distribution $\widetilde{P}_c(f_s)$ of the static friction force thresholds of the contacts. If a given contact has an area A, then it is characterized by the static friction threshold $f_s \propto A$ and the (shear) elastic constant $k \propto \sqrt{A}$ (assuming that the linear size of the contact and its height are of the same order of magnitude, see [16] and Appendix A in Ref. [18]). The displacement threshold for the given contact is $x_s = f_s/k$, so that $f_s \propto x_s^2$, or $df_s/dx_s \propto x_s$. Then, using $P_c(x_s)\, dx_s = \widetilde{P}_c(f_s)\, df_s$, we obtain $P_c(x_s) \propto x_s \widetilde{P}_c[f_s(x_s)]$, or

$$P_c(x) \propto x^{1+2n} \exp(-x^2/x_*^2)\,, \qquad (8)$$

where x_* may be estimated from experiments as $N_c k x_* \approx F_s$. In the SFA/B (surface force apparatus/balance) experiments, where the sliding surfaces are made of mica, the interface may be atomically flat over a macroscopic area. But even in this case the lubricant film cannot be ideally homogeneous throughout the whole contact area — it should be split into domains, e.g., with different orientation, because this will lower the system free energy due to the increase of entropy. Domains of different orientations have different values for the thresholds f_{si}, i.e., they play the same role as asperities in the contact of rough surfaces.

For the normalized distribution of static thresholds given by Eq. (8) with $n = 1$,

$$P_c(x) = (2/x_*)\, u^3 e^{-u^2}\,, \quad \text{where} \quad u \equiv x/x_*\,, \qquad (9)$$

we can express the steady-state solution of the master equation analytically. In this case

$$J_c(x) = (1 + u^2)\, e^{-u^2}\,, \qquad (10)$$

so that at zero temperature we have

$$P(x) = (2/x_*)\, u^3/(1 + u^2)\,, \qquad (11)$$

$$U(x) = u^2 - \ln(1 + u^2)\,, \qquad (12)$$

$$E_P(x) = J_c(x) = (1 + u^2)\, e^{-u^2}\,, \qquad (13)$$

$$C[P] = x_*/C_0\,, \quad \text{where} \quad C_0 = \frac{4}{3\sqrt{\pi}} \approx 0.752\,, \qquad (14)$$

$$Q(x) = (C_0/x_*)(1 + u^2)\, e^{-u^2}\,, \quad u \geq 0 \qquad (15)$$

and the kinetic friction is

$$f_k \equiv F_k/(N_c k) = f_{k0} \equiv C_0 x_*\,. \qquad (16)$$

The ME formalism described above can be extended to take into account various generalizations of the EQ model, such as temperature effects and contact aging, which are examined in the following sections.

III. NONZERO TEMPERATURE

Temperature effects enter in the ME formalism through their effect on the fraction of contacts that break per unit displacement of the sliding block, $P(x)$, because thermal fluctuations allow an activated breaking of any contact which is still below the threshold [16, 18, 20–23]. For a sliding at velocity v so that $X = vt$, the thermally activated jumps can be incorporated in the master equation, if we use, instead of the zero-temperature breaking fraction density $P(x)$, an expression $P_T(x)$ defined by (see [18])

$$P_T(x) = P(x) + H(x)\,, \qquad (17)$$

where the temperature contribution is given by

$$H(x) = \frac{\omega}{v}\, e^{kx^2/2k_B T} \int_x^\infty d\xi\, P_c(\xi)\, e^{-k\xi^2/2k_B T} \qquad (18)$$

for "soft" contacts or by

$$H(x) = \frac{\omega}{v} \int_x^\infty d\xi\, P_c(\xi) \left(1 - \frac{x}{\xi}\right)^{\frac{1}{2}} e^{-k\xi^2\left(1 - \frac{x}{\xi}\right)^{\frac{3}{2}}/2k_B T} \qquad (19)$$

in the case of "stiff" contacts which have a deep pinning potential so that their breaking only occurs with a significant probability when their stretching is close to the threshold. Here ω is the attempt frequency of contact breaking, $\omega \sim 10^{10}$ s^{-1} according to Refs. [16, 21].

For concreteness, in what follows we assume that the contacts are soft, Eq. (18), and we select $n = 1$ in Eq. (8), so that $P_c(x)$ is given by Eq. (9).

At a nonzero temperature the total rate of contact breaking, Eq. (17), is equal to $P_T(x) = P(x) + (\omega/v)\, h(x)$, where for the soft contacts

$$h(x) = \frac{1 + (1 + b)\, u^2}{(1 + b)^2}\, e^{-u^2} \qquad (20)$$

with

$$b(T) = \frac{kx_*^2}{2k_B T}\,. \qquad (21)$$

The condition $b = 1$ defines a crossover temperature

$$k_B T_* = \frac{1}{2} k x_*^2 . \qquad (22)$$

Then, a straightforward integration gives the function $U_T(x) = \int_0^x d\xi \, P_T(\xi) = U(x) + \Delta U(x)$, where

$$\Delta U(x) = S_0(v, T) \left[\mathrm{erf}(u) - S_1(T) \, u \, e^{-u^2} \right] \qquad (23)$$

with

$$S_0(v, T) = \frac{\omega x_*}{C_0 v} \frac{(1 + b/3)}{(1 + b)^2} \qquad (24)$$

and

$$S_1(T) = \frac{C_0}{2} \frac{(1 + b)}{(1 + b/3)} . \qquad (25)$$

The coefficient $S_1(T)$ weakly changes with temperature from $S_1(0) = 2/\sqrt{\pi} \approx 1.128$ to $S_1(\infty) = C_0/2 \approx 0.376$. On the other hand, the coefficient $S_0(v, T)$ determines whether the effect of temperature is essential or not. The temperature-induced breaking of contacts is essential at low driving velocities only, when $S_0(v, T) \gg 1$. Thus, the equation $S_0(v_*, T) = 1$ defines the crossover velocity:

$$v_*(T) = \frac{\omega x_*}{C_0} \frac{[1 + b(T)/3]}{[1 + b(T)]^2} . \qquad (26)$$

We see that v_* monotonically increases with temperature as $v_*(T) \approx 0.443 \, \omega x_* T / T_*$ at $T \ll T_*$ and approaches the maximal value $v_* \approx 1.33 \, \omega x_*$ at $T \gg T_*$.

Then, $E_{PT}(x) = e^{-U_T(x)} = (1 + u^2) \, e^{-u^2} e^{-\Delta U(x)}$, and we can find the kinetic friction force:

$$f_k(v, T) = \int_0^\infty dx \, x \, E_{PT}(x) \bigg/ \int_0^\infty dx \, E_{PT}(x) . \qquad (27)$$

At a low driving velocity, $v \ll v_*$, we may put $\Delta U(x) \approx S_2 u$, where

$$S_2(v, T) = \frac{\omega x_*}{v (1 + b)^2} , \qquad (28)$$

and Eq. (27) leads to

$$f_k \approx x_*/S_2 = (v/\omega)(1 + b)^2. \qquad (29)$$

A linear dependence of the kinetic friction on the driving velocity at low velocities corresponds to the creep motion due to temperature activated breaking of contacts and was predicted in several earlier studies [16, 21–23], although our approach allowed us to derive it rigorously. The dependence (29) may be interpreted as an effective "viscosity" of the confined interface:

$$\eta = \frac{f_k}{v} = \frac{1}{\omega} \left(1 + \frac{k x_*^2}{2 k_B T} \right)^2 . \qquad (30)$$

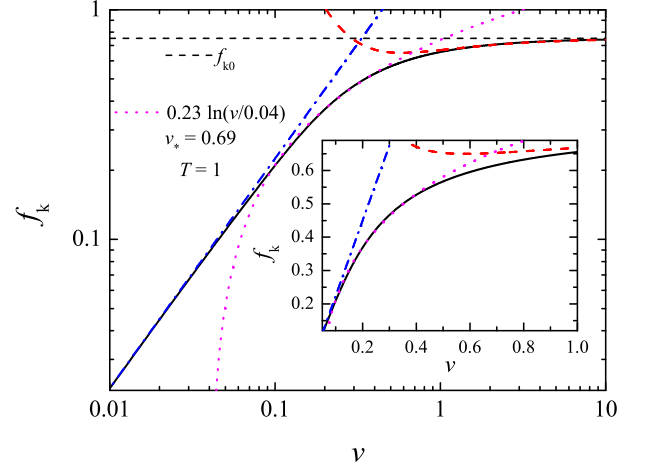FIG. 1: (Color online): The friction force f_k as a function of the driving velocity. Dash-dotted blue line shows the low-v approximation (29), dashed red line shows the high-v approximation (31), and dotted magenta line shows a logarithmic fitting. $k = 1$, $\omega = 1$, $x_* = 1$, $k_B T = 1$.

At a high velocity, $v \gg v_*$, when $e^{-\Delta U(x)} \approx 1 - S_2 u + \frac{1}{2}(S_2 u)^2$, we obtain $C \approx 3\sqrt{\pi}/4 - S_2 + (5\sqrt{\pi}/16)S_2^2$ so that

$$f_k \approx f_{k0} \left(1 - C_1 S_2 + C_2 S_2^2 \right), \qquad (31)$$

where $C_1 = 5\sqrt{\pi}/8 - C_0 \approx 0.356$ and $C_2 = 16/9\pi - 1/3 \approx 0.233$. Equation (31) agrees qualitatively with that found by Persson [16] in the case of $b \gg 1$.

Approximate expressions (29, 31) together with the numerical integration of Eq. (27) are presented in Fig. 1. Also we showed a logarithmic fitting which operates in a narrow interval of velocities near the crossover velocity only. Persson [16] showed that the logarithmic dependence may be obtained analytically, only if the $P_c(x)$ distribution has a sharp cutoff at some $x = x_s$ as, e.g., in simplified versions of the EQ model with $P_c(x) = \delta(x - x_s)$.

Although we cannot obtain analytical results for the stiff contacts, we calculated the $f_k(v)$ dependences numerically (see Fig. 2), which shows that the effect remains qualitatively the same.

IV. AGING OF CONTACTS

The aging of contacts was considered in our work [18] where, however, we ignored the temperature-induced breaking of contacts discussed above in Sec. III. When aging is taken into account the master equation for $Q(x, X)$ must be completed by an equation for the evolution of $P_c(x)$, which in turns affects $P(x)$. Let the newborn contacts be characterized by a distribution $P_{ci}(x)$, while at $t \to \infty$, due to aging the distribution $P_c(x)$ approaches a final distribution $P_{cf}(x)$. If we assume that
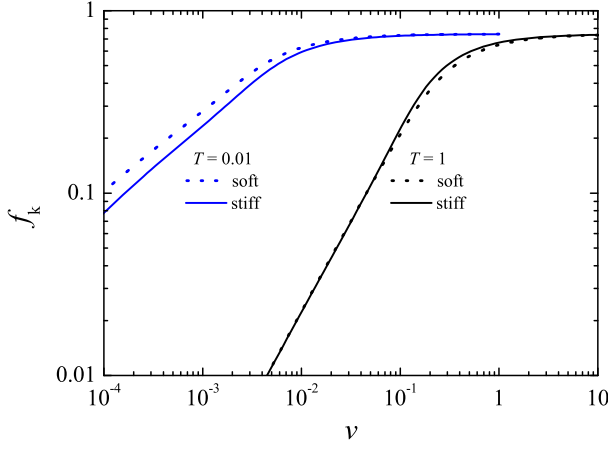
FIG. 2: (Color online): The friction force f_k as a function of the driving velocity v for soft (dotted) and stiff (solid curves) contacts at low temperature $k_B T = 0.01$ (blue) and high temperature $k_B T = 1$ (black). $k = 1$, $\omega = 1$, $x_* = 1$.

the evolution of $P_c(x)$ corresponds to a stochastic process, then it should be described by a Smoluchowsky equation

$$\frac{\partial P_c}{\partial t} = D\,\widehat{L}P_c, \quad \text{where} \quad \widehat{L} \equiv \frac{\partial}{\partial x}\left(B(x) + \frac{\partial}{\partial x}\right), \quad (32)$$

in which the "diffusion" parameter D describes the rate of aging, $B(x) = d\bar{U}(x)/dx$, and the "potential" $\bar{U}(x)$ determines the final distribution, $P_{cf}(x) \propto \exp\left[-\bar{U}(x)\right]$, so that we can write

$$B(x) = -\left[dP_{cf}(x)/dx\right]/P_{cf}(x). \quad (33)$$

However, because the contacts continuously break and form again when the substrate moves, this introduces two extra contributions in the equation determining $\partial P_c/\partial X$ in addition to the pure aging effect described by Eq. (32): a term $P(x;X)Q(x;X)$ takes into account the contacts that break, while their reappearance with the threshold distribution $P_{ci}(x)$ gives rise to the second extra term in the equation. Thus, the evolution of P_c is described by the equation

$$\frac{\partial P_c(x;X)}{\partial X} - D_v\widehat{L}P_c(x;X) + P(x;X)\,Q(x;X)$$
$$= P_{ci}(x)\,\Gamma(X), \quad (34)$$

where $D_v = D/v$, and $v = dX(t)/dt$ is the driving velocity. Finally, we come to the set of equations (1–3, 34). For the steady-state regime, Eq. (34) reduces to

$$D_v C[P]\,\widehat{L}P_c(x) = P(x)\,E_P(x) - P_{ci}(x), \quad (35)$$

where we used Eqs. (5) and (6). Taking also into account the identity $P(x)\,E_P(x) = P_c(x)$ [18], we finally come to the equation

$$D_v C[P]\,\widehat{L}P_c(x) = P_c(x) - P_{ci}(x). \quad (36)$$
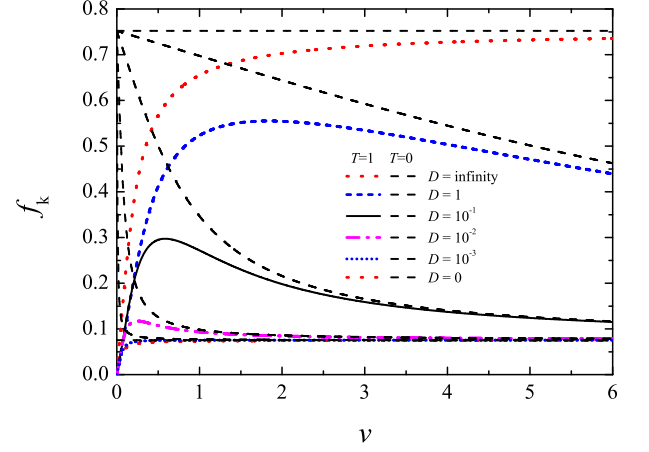

FIG. 3: (Color online): The kinetic friction force f_k as a function of the driving velocity v for different values of the aging rate: $D = \infty$ (red dotted), 1 (blue short-dashed), 10^{-1} (black solid), 10^{-2} (magenta dash-dotted), 10^{-3} (blue short-dotted), and $D = 0$ (red dotted curve). $k = 1$, $\omega = 1$, $k_B T = 1$; the initial and final $P_c(x)$ distributions are given by Eq. (9) with $x_{*i} = 0.1$ and $x_{*f} = 1$ correspondingly. Dashed curves shows the dependences at $T = 0$.

It was shown [18] that the kinetic friction monotonically decreases with the driving velocity as $F_k(v) - F_k(0) \propto -v/D$ in the low-velocity limit and $F_k(v) - F_k(\infty) \propto D/v$ in the high-velocity case. One may expect that at low velocities this decreasing will compensate the friction increasing due to temperature induced jumps. The problem, however, is more involved.

When the temperature effects are incorporated, Eq. (36) for the function $P_c(x)$ in the steady state takes the form

$$D_v\,C[P_T]\,\widehat{L}P_c(x) = P_c(x) - P_{ci}(x). \quad (37)$$

Numerical solutions of Eq. (37) are presented in Figs. 3 and 4a: the initial increase of the kinetic friction F with the driving velocity v due to the temperature activated breaking of contacts is followed by the decrease of F due to contacts aging. Figure 4b shows also the dependence of the effective "viscosity" $\eta = f_k/v$ on the driving velocity v. It is constant at low velocity and then decreases; the latter may be approximately fitted by a power law $\eta(v) \propto v^{-\alpha}$ with the exponent α changing from 1.5 to 1 as D decreases.

Using the definition (32) of the operator $\widehat{L}$ and Eq. (33) for the function $B(x)$, the l.h.s. of Eq. (37) may be rewritten as

$$D_v C\,\widehat{L}P_c(x) = D_v C\,\frac{d}{dx}\left(P_{cf}(x)\,\frac{d}{dx}\frac{P_c(x)}{P_{cf}(x)}\right), \quad (38)$$

while the r.h.s. of Eq. (37) may be presented as

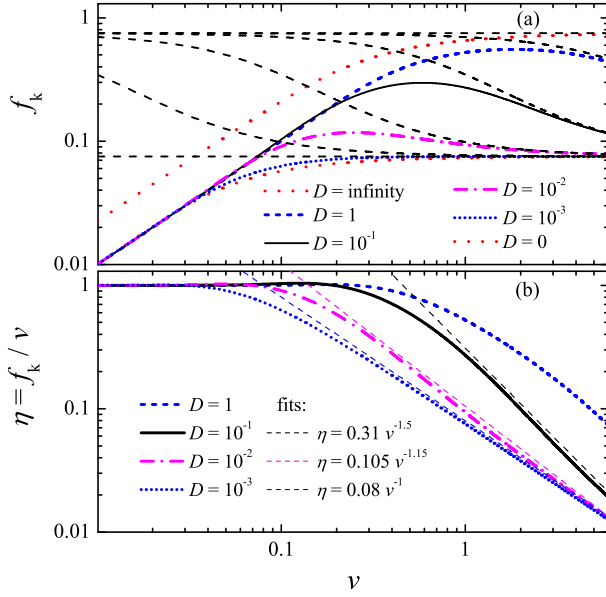$$P_c(x) - P_{ci}(x) = -\frac{d}{dx}\left[J_c(x) - J_{ci}\right], \quad (39)$$

FIG. 4: (Color online): (a) The same as in Fig. 3 in log-log scale. (b) The dependences of the effective "viscosity" $\eta = f_k/v$ on the velocity v (dashed lines show power-law fits).

where $J_{ci}(x) = \int_x^\infty d\xi\, P_{ci}(\xi)$. Using Eqs. (38) and (39), we can find the first integral of Eq. (37):

$$D_v\, C[P_T]\, P_{cf}(x) \frac{d}{dx}\left(\frac{P_c(x)}{P_{cf}(x)}\right) = J_{ci}(x) - J_c(x). \quad (40)$$

Integration of Eq. (40) leads to an integral equation for the function $P_c(x)$:

$$P_c(x) = P_{cf}(x)\left\{1 + \frac{v}{DC[P_T]}\int_0^x \frac{J_{ci}(\xi) - J_c(\xi)}{P_{cf}(\xi)}\, d\xi\right\}. \quad (41)$$

Substituting $J_c(x) \approx J_{cf}(x) = \int_x^\infty d\xi\, P_{cf}(\xi)$ into the r.h.s. of Eq. (41), one may analytically find the low-velocity behavior of the kinetic friction, for example, the decrease of f_k with v for $T = 0$. At a nonzero temperature, however, aging does not affect the low-velocity behavior (29) and only reduces the interval of velocities where Eq. (29) is valid, as demonstrated in Figs. 3 and 4. Indeed, at $v \to 0$ and $T > 0$ the main contribution to $P_T(x)$ comes from the function $H(x) \propto \omega/v$ in Eq. (17), which only weakly depends on $P_c(x)$.

The limit $D_v = D/v \to 0$ may be studied with the help of Eq. (37) by substituting $P_c(x) \approx P_{ci}(x)$ into its left-hand side. For the function (9), this approach gives

$$P_c(x) - P_{ci}(x) \approx -\frac{16 D_v C[P]}{x_{*i} x_{if}^2}\, u_i e^{-u_i^2}\left(1 - \frac{1}{2}u_i^2\right) \quad (42)$$

and

$$J_c(x) - J_{ci}(x) \approx \frac{4 D_v C[P]}{x_{if}^2}\, u_i^4 e^{-u_i^2}, \quad (43)$$
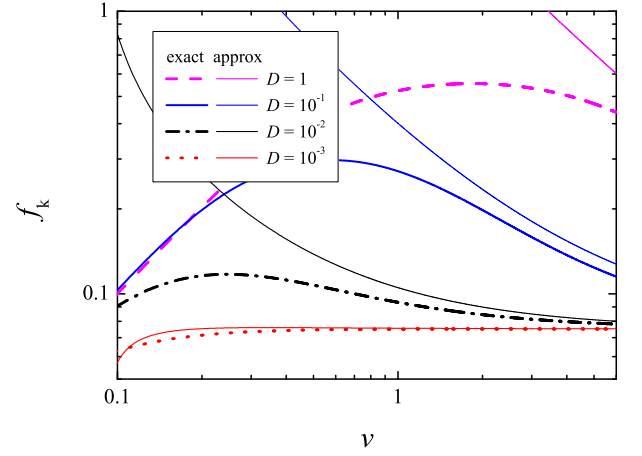

FIG. 5: (Color online): The kinetic friction force f_k as a function of the driving velocity v for different values of the aging rate $D = 1$ (magenta dashed), 10^{-1} (blue solid), 10^{-2} (black dash-dotted) and 10^{-3} (red dotted curve) as compared with approximate expressions (thin solid curves). $k = 1$, $\omega = 1$, $k_B T = 1$; the initial and final $P_c(x)$ distributions are given by Eq. (9) with $x_{*i} = 0.1$ and $x_{*f} = 1$ correspondingly.

where $u_i = x/x_{*i}$ and

$$\frac{1}{x_{if}^2} = \frac{1}{x_{*i}^2} - \frac{1}{x_{*f}^2}. \quad (44)$$

Then, taking the corresponding integrals, we obtain to first order in v^{-1}

$$C \approx x_{*i}\left(C_0^{-1} - S_2 + C_{12} S_3\right) \quad (45)$$

and

$$f_k \approx \frac{x_{*i}^2}{C}\left[1 - (C_0 + C_1)S_2 + \widetilde{C}_{12} S_3\right], \quad (46)$$

where

$$S_3(v) = 4 D_v C[P]/x_{if}^2, \quad (47)$$

$C_{12} \approx 1.324$ and $\widetilde{C}_{12} \approx 1.789$ are numerical constants. A comparison of the exact and approximate expressions is shown in Fig. 5.

V. DELAY IN CONTACT FORMATION

Finally, let us take into account the delay in contact formation following the work of Schallamach [22]. Let τ be the delay time, N be the total number of contacts, N_c be the number of coupled (pinned) contacts, and $N_f = N - N_c$ be the number of detached (sliding) contacts. The fraction of contacts that detach per unit displacement of the sliding block is $\Gamma(v, T) = \int dx\, P(x)\, Q(x)$, i.e., when the slider shifts by ΔX, the number of detached contacts changes by $N_c \Gamma \Delta X$, so that $N_f = \Gamma v \tau N_c$. Using $N_c + N_f = N$, we obtain $N_c = N/(1 + \Gamma v \tau)$ and
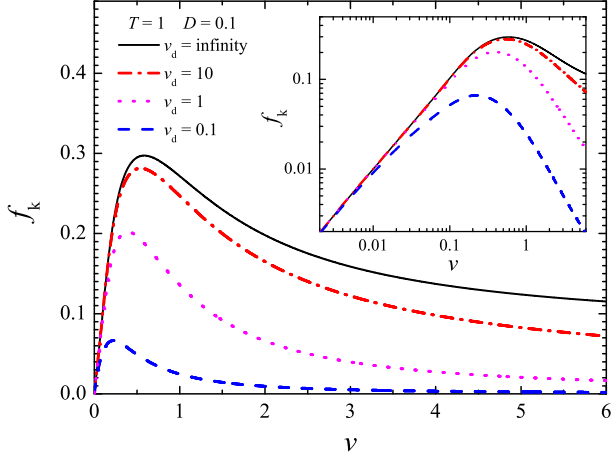
FIG. 6: (Color online): The kinetic friction force f_k as a function of the driving velocity v for different values of the delay time: $v_d = \infty$ (black solid), 10 (red dot-dashed), 1 (magenta dotted) and 0.1 (blue dashed curve) for $D = 0.1$ and $k_B T = 1$ (other parameters as in Fig. 3). Inset shows the same in log-log scale.

$N_f = N\Gamma v\tau/(1 + \Gamma v\tau)$. If we define $\bar{x} = 1/\Gamma$ and $v_d = \bar{x}/\tau$, we can write

$$N_c = \frac{N}{1 + v/v_d} \quad \text{and} \quad N_f = \frac{Nv/v_d}{1 + v/v_d} . \qquad (48)$$

The coupled contacts produce the force f_k defined above by the steady-state solution of the master equation. The combined dependence which incorporates temperature effects, aging and delay in contact formation, is shown in Fig. 6 for different values of the parameter v_d.

However, above we assumed that the sliding contacts experience zero friction, while these contacts may experience a viscous friction force $f_l = \eta_l v$, where η_l corresponds to the (bulk) viscosity of the liquid lubricant. In this case the kinetic friction should be additionally multiplied by a factor $\beta(v) = 1 + v^2/v_\eta v_d$, where $v_\eta = f_k/\eta_l$ ($v_\eta \gg v_d$). Such a correction may be expected at huge velocities only, e.g., for $v \sim 1$ m/s. In this case the function $F_k(v)$, after decreasing, reaches a minimum at a velocity $v_0 \approx (v_\eta v_d)^{1/2}$, and then increases according to a law $f_k(v) \propto \eta_l v$. Note that the viscous friction which comes from the excitation of phonons in the substrates, as shown in MD simulation [7], may also depend on the velocity, e.g., as $\eta_l \propto v^4$.

VI. MAKING THE LINK WITH EXPERIMENTS

For a real system, the results presented in the previous sections allow the calculation of the kinetic friction force $F_k(v, T)$ provided the parameters of the model are known. In this section section we examine how they can be evaluated from experiments.

The contact parameters k and ω may be estimated with the help of elastic theory [28]. Let us assume that a contact has a cylinder shape of height h (the thickness of the interface) and radius r_c, so that it is characterized by the section $A_i = \pi r_c^2$, the (geometrical) inertial momentum $I = \pi r_c^4/4$, a mass density ρ and a Young modulus E. If the cylinder foot is fixed and a force Δf is applied to its top, the latter will be shifted on the distance $\Delta x = \Delta f h^3/3EI$ (the problem of bending pivot, see Sec. 20, example 3 in Ref. [28]). Thus, the effective elastic constant of the contact is $k = \Delta f/\Delta x = 3EI/h^3$. The minimal frequency of bending vibration of the pivot with one fixed end and one free end, is given by $\omega \approx (3.52/h^2)(EI/\rho A_i)^{1/2}$ (see Sec. 25, example 6 in Ref. [28]).

Next, let a be the average distance between the contacts, so that the total area of the interface is $A = Na^2$, and introduce the dimensionless parameter $\gamma_c = r_c/a$ ($\gamma_c < 0.5$). The threshold distance x_* may be estimated as follows. At the beginning, when all contacts are in the unstressed state, the maximal force the slider may sustain is equal to $F_* \approx Nkx_*$ (this force corresponds to the first large stick spike in the $F(t)$ dependence at the beginning of stick-slip motion at low driving). Thus, we obtain that $kx_* \approx a^2\sigma_*$, where $\sigma_* = F_*/A$ is the maximal shear stress.

Let us consider a contact of two rough surfaces and assume that $a = h = r_c$. Then we obtain

$$\omega \approx \frac{1.76\sqrt{E/\rho}}{r_c} \qquad (49)$$

for the attempt frequency,

$$k = (3\pi/4)Er_c \qquad (50)$$

for the contact elasticity, and

$$x_* = r_c^2\sigma_*/k \qquad (51)$$

for the threshold distance. For steel substrates we may take $\rho = 10^4$ kg/m^3 for the mass density, $E = 2 \times 10^{11}$ N/m^2 for the Young modulus, and $\sigma_c = 10^9$ N/m^2 for the plasticity threshold. Assuming that $\sigma_* = \sigma_c$ and $r_c \approx 1$ μm, we find that $\omega \approx 7.9 \times 10^9$ s^{-1}, $k \approx 4.7 \times 10^5$ N/m, $x_* \approx 2.1 \times 10^{-9}$ m, $b \approx 2.7 \times 10^8$ for room temperature (i.e., $b \gg 1$), so that the crossover velocity is quite low, $v_* \approx 0.03$ μm/s.

Now let us consider a lubricated system, e.g., the one with a few OMCTS layers as studied by Klein [29] and Bureau [27], and assume that the lubricant consists of solidified islands which melt under stress as proposed by Persson [25]. In this case, instead of using the Young modulus, let us assume that $x_* = r_c$; this allows us to find the parameter $EI = ah^3\sigma_*/3\gamma_c$. Then, the elastic constant is $k = a\sigma_*/\gamma_c$, the attempt frequency is

$$\omega \approx 1.15 \sqrt{\sigma_*/ah\rho\gamma_c^3} , \qquad (52)$$

the parameter b is given by

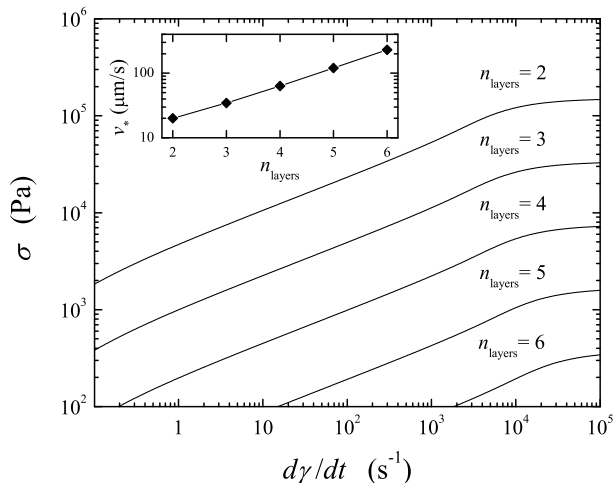$$b \approx \gamma_c a^3\sigma_*/2k_B T , \qquad (53)$$

FIG. 7: The shear stress σ as a function of the shear rate $\dot{\gamma}$ for different values of the OMCTS film thickness from $n_l = 2$ to 6 monolayers. Inset: the crossover velocity v_* as a function of the number of layers.

and in the case of $b \gg 1$ the crossover velocity is

$$v_* \approx \gamma_c \omega a / 3 C_0 b \approx k_B T / \sqrt{a^5 h \rho \sigma_* \gamma_c^3} \,. \qquad (54)$$

For a four-layer OMCTS film [29] one may take $\rho = 956$ kg/m^3, $h \approx 3.5 \times 10^{-9}$ m, $F_* \approx 2 \times 10^{-5}$ N and $A \approx 10^{-10}$ m^2 so that $\sigma_* \approx 2 \times 10^5$ Pa. Assuming $\gamma_c = 0.5$ and $a \approx 1$ μm, we obtain for room temperature, $k_B T = 4 \times 10^{-21}$ J, that $\omega \approx 8 \times 10^8$ s^{-1} and $b \approx 1.25 \times 10^7$, i.e. this system is in the low-temperature limit too, although the crossover velocity is much higher than for rough surfaces, $v_* \approx 16$ μm/s.

Moreover, we may calculate the dependence $f_k(v)$ for different thicknesses of the lubricant film. If the film consists of n_l layers, then the film thickness is $h = n_l d$, where $d \approx 8.75$ Å is the diameter of the OMCTS molecule. Let us assume that the maximal shear stress exponentially decreases with the number of layers according to the results of MD simulation [7], $\sigma_* = \sigma_0 e^{-\beta n_l}$, where $\beta \sim 1$ is a numerical constant. Taking $\sigma_0 = 4 \times 10^6$ N/m^2 and $\beta = 1.5$, we obtain the dependences of the shear stress $\sigma = F_k / A$ on the shear rate $\dot{\gamma} = v/h$ shown in Fig. 7, which may be compared with the experimental dependences (Fig. 2a) of Bureau [27].

Note that our approach may overestimate the value of the crossover velocity v_*. First, the crossover will occur earlier if the delay and/or aging effects play a significant role. Besides, at low temperatures the stiff contacts lead to higher "viscosity" and lower values of v_* than the soft contacts considered above (see Fig. 2). Second, we completely ignored the elastic interaction between the contacts. If the latter would be incorporated, a breaking of one contact may stimulate neighboring contacts to break as well, i.e., the value of the parameter a should describe such a cooperative "contact" size which may be much larger than those of individual ones.

Giving a quantitative evaluation of the influence of aging on the velocity dependence of the friction coefficient is harder than for the temperature dependence due to insufficient experimental data. Aging appears to cause a decrease of friction as velocity increases, and thus, when such a behavior is observed experimentally [9, 13] it can be considered as a strong indication of the presence of aging. Our analysis indicates that the combined effect of temperature and aging leads to a maximum in the friction coefficient versus velocity. Therefore, when aging is manifested by a decreasing friction versus velocity, extending the experiments to lower velocities and temperatures might detect the maximum and thus provide some quantitative data to evaluate the aging parameters.

Although the aim of our work was to find the dependence of the kinetic friction on the driving velocity, our approach allows us to find the dependence on temperature as well. However, the behavior of a real tribological system is more involved, because all parameters may depend on temperature T in a general case. For example, the delay time τ may exponentially depend on T if the formation of a new contact is an activated process [22]; the same may be true for the aging rate D. In this case one may obtain a nonmonotonic temperature dependence of friction with, e.g., a peak at cryogenic temperatures [21].

VII. CONCLUSION

In this study we determined the dependence of the kinetic friction force in the smooth sliding regime on the driving velocity. In a general case, the friction linearly increases with the velocity (this creep motion may be interpreted as an effective "viscosity" of the confined film), passes through a maximum and then decreases due to delay/aging effects. The decay may be followed by a new growth in friction in the case of liquid lubricant. Estimation showed that for the contact of rough surfaces, the initial growth of friction should occur at quite low velocities, $v \ll 0.1$ μm/s, so that for typical velocities the friction is independent on velocity in agreement with the Coulomb law. However, for the case of lubricated friction with a thin lubricant film which solidifies due to compression, the $f_k(v)$ dependence is essential, and the linear dependence may stay valid up to velocities $v \sim 10 \div 10^3$ μm/s. At higher velocities the growth saturates and the $f_k(v)$ dependence may be fitted by a logarithmic law. The latter velocity interval is narrow if the distribution of static thresholds is wide; the logarithmic law may be found analytically for a wide interval of velocities when the thresholds are approximately identical, i.e., for the singular distribution $P_c(x) = \delta(x - x_s)$.

We emphasize that our approach is only valid for a system with many contacts, for example, $N > 20$ at least [21]. When the contact is due to a single atom as it may occur in the AFM/FFM devices, the friction can be accurately described by the Prandtl-Tomlinson

model and should follow the logarithmic $f_k(v)$ dependence, $f_k(v) \propto (\ln v/v_0)^{2/3}$ [30]. But if the AFM/FFM tip is not too sharp so that the contact is due to more than one atom, the logarithmic dependence is only approximate and, moreover, for some systems the friction may decrease with the velocity which has to be attributed to the aging/delay effects [8, 9, 31].

In this work we had in mind that contacts correspond to real asperities in the case of the contact of rough surfaces or to "solid islands" for the lubricated interface. However, the ME approach also operates when the contact is due to long molecules which are attached by their ends to both substrates. Such a system was first studied by Schallamach [22] and then further investigated by Filippov *et al.* [20], Srinivasan and Walcott [23], and Barel *et al.* [21]. Note that when all molecules are identical, they are characterized by the same static threshold, i.e., this system is close to the singular one, where the logarithmic $f_k(v)$ dependence has to have a wide interval of operation.

Finally, let us discuss restrictions of our approach. First of all, we assumed the somehow idealized case of wearless friction; wearing may mask the predicted dependences. Besides, the interface is heated during sliding; this effect is hard to describe analytically as well as to control experimentally. Then, we did not estimated the delay/aging parameters; moreover, these parameters, e.g., the delay time τ, may depend on the driving velocity v. Besides, we assumed the simplest mechanism of aging described by the Smoluchowsky equation, while the real situation may be more involved, e.g., it may correspond to the Lifshitz-Slözov mechanism [18]. Also, we assumed that the reformed contacts appear in the unstressed state, $R(x) = \delta(x)$ in Eq. (1), which may not be the case in real systems.

The most important issue, however, is the incorporation of the elastic interaction between the contacts as well as elastic deformation of substrates at sliding. This point certainly deserves a detailed investigation and is the topic of our future work.

Acknowledgments

[1] D. Dowson, *History of tribology* (Longman, New York, 1979).

[2] B.N.J. Persson, *Sliding friction: Physical principles and applications* (Springer-Verlag, Berlin, 1998).

[3] M.O. Robbins and M.H. Müser, in *Handbook of modern tribology*, edited by B. Bhushan (CRC Press, Boca Raton, 2000).

[4] M.O. Robbins, in *Jamming and rheology: Constrained dynamics on microscopic and macroscopic scales*, edited by A.J. Liu and S.R. Nagel (Taylor and Francis, London, 2000).

[5] B.N.J. Persson, O. Albohr, F. Mancosu, V. Peveri, V.N. Samoilov, and I.M. Sivebaek, Wear **254**, 835 (2003); I.M. Sivebaek, V.N. Samoilov, and B.N.J. Persson, Langmuir **26**, 8721 (2010).

[6] T. Baumberger and C. Caroli, Advances in Physics **55**, 279 (2006).

[7] O.M. Braun and A.G. Naumovets, Surf. Sci. Reports **60**, 79 (2006).

[8] W. Hild, S.I-U. Ahmed, G. Hungenbach, M. Scherge, and J.A. Schaefer, Tribology Lett. **25**, 1 (2007).

[9] J. Chen, I. Ratera, J.Y. Park, and M. Salmeron, Phys. Rev. Lett. **96**, 236102 (2006).

[10] C. Marone, Ann. Rev. Earth. Planet. Sci. **26**, 643 (1988).

[11] T. Bouhacina, J.P. Aim, S. Gauthier, D. Michel and V. Heroguez, Phys. Rev. B **56** 7694 (1997).

[12] E. Gnecco, R. Bennewitz, T. Gaylog, Ch. Loppacher, M. Bammerlin, E. Meyer and H.J. Gntherodt, Phys. Rev. Lett. **84**, 1172 (2000).

[13] A. Schirmeisen, L. Jansen, H. Hlscher and H. Fuchs, App. Phys. Lett. **88**, 123108 (2006).

[14] R. Burridge and L. Knopoff, Bull. Seismol. Soc. Am. **57**, 341 (1967).

[15] Z. Olami, H.J.S. Feder, and K. Christensen, Phys. Rev. Lett. **68**, 1244 (1992).

[16] B.N.J. Persson, Phys. Rev. B **51**, 13568 (1995).

[17] O.M. Braun and M. Peyrard, Phys. Rev. Lett. **100**, 125501 (2008).

[18] O.M. Braun and M. Peyrard, Phys. Rev. E **82**, 036117 (2010).

[19] O.M. Braun and J. Röder, Phys. Rev. Lett. **88**, 096102 (2002).

[20] A.E. Filippov, J. Klafter, and M. Urbakh, Phys. Rev. Lett. **92**, 135503 (2004).

[21] I. Barel, M. Urbakh, L. Jansen, and A. Schirmeisen, Phys. Rev. Lett. **104**, 066104 (2010).

[22] A. Schallamach, Wear **6**, 375 (1963).

[23] M. Srinivasan and S. Walcott, Phys. Rev. E **80**, 046124 (2009).

[24] J.A. Greenwood and J.B.P. Williamson, Proc. Roy. Soc. A **295**, 300 (1966).

[25] B.N.J. Persson, Phys. Rev. B **48**, 18140 (1993).

[26] O.M. Braun and N. Manini, Phys. Rev. E **?**, ? (2011) [article EM10550]; arXiv:1101.5508.

[27] L. Bureau, Phys. Rev. Lett. **104**, 218302 (2010).

[28] L.D. Landau and E.M. Lifshitz, *Theory of Elasticity* (Pergamon, Oxford, 1970).

[29] J. Klein, Phys. Rev. Lett. **98**, 056101 (2007).

[30] L. Jansen, H. Hölscher, H. Fuchs, and A. Schirmeisen, Phys. Rev. Lett. **104**, 256101 (2010).

[31] E. Riedo, E. Gnecco, R. Bennewitz, E. Meyer, and H. Brune, Phys. Rev. Lett. **91**, 084502 (2003).